Author Manuscript Published OnlineFirst on December 26, 2013; DOI: 10.1158/0008-5472.CAN-13-1750
Author manuscripts have been peer reviewed and accepted for publication but have not yet been edited.

Phosphorylation at Ser-181 of oncogenic KRAS is required for tumor growth

Carles Barceló[a*], Noelia Paco[a*], Mireia Morell[b], Blanca Alvarez-Moya[a,d], Neus Bota-Rabassedas[a,e], Montserrat Jaumot[a], Felip Vilardell[c], Gabriel Capella[b] and Neus Agell[a,1]

[a]Departament de Biologia Cel•lular, Immunologia i Neurociències, Institut d'Investigacions Biomèdiques August Pi i Sunyer (IDIBAPS), Facultat de Medicina. Universitat de Barcelona, C/ Casanova 143, 08036 Barcelona, Spain

[b]Hereditary Cancer Program, Translational Research Laboratory, Catalan Institute of Oncology, ICO-IDIBELL, Hospitalet de Llobregat, Barcelona, Spain; Gran Via 199-203, 08907- L'Hospitalet de Llobregat Spain

[c] Servei d'Anatomia Patològica i Institut de Recerca Biomèdica de Lleida, Avda. Rovira Roure, 80, 25198 Lleida.

[d] Present address: IFOM-IEO Campus, Milan, Italy

[e] Present address: IBE, CSIC-UPF, Barcelona, Spain

*Both authors contributed equally to this work

[1]**Corresponding author**: Neus Agell, Dept. Biologia Cel·lular, Immunologia i Neurociències, Facultat de Medicina, Universitat de Barcelona, C/Casanova 143, 08036 Barcelona, Spain; Phone# 34934036257;e-mail: neusagell@ub.edu.

Running title: KRAS phosphorylation promotes tumor growth

Keywords: KRAS, tumorogenesis, phosphorylation, PKC

Grant support: This study was supported by MICINN-Spain [SAF2010-20712]

Conflict of interest: none

Word count : 5150

Number of figures: 7

Downloaded from cancerres.aacrjournals.org on January 7, 2014. © 2013 American Association for Cancer Research.

Author Manuscript Published OnlineFirst on December 26, 2013; DOI: 10.1158/0008-5472.CAN-13-1750
Author manuscripts have been peer reviewed and accepted for publication but have not yet been edited.

Abstract

KRAS phosphorylation has been reported recently to modulate the activity of mutant KRAS protein in vitro. In this study, we defined S181 as a specific phosphorylation site required to license the oncogenic function of mutant KRAS in vivo. The phosphomutant S181A failed to induce tumors in mice, whereas the phosphomimetic mutant S181D exhibited an enhanced tumor formation capacity, compared to the wild-type KRAS protein. Reduced growth of tumors composed of cells expressing the non-phosphorylatable KRAS S181A mutant was correlated with increased apoptosis. Conversely, increased growth of tumors composed of cells expressing the phosphomimetic KRAS S181D mutant was correlated with increased activation of AKT and ERK, two major downstream effectors of KRAS. Pharmacological treatment with PKC inhibitors impaired tumor growth associated with reduced levels of phosphorylated KRAS and reduced effector activation. In a panel of human tumor cell lines expressing various KRAS isoforms, we showed that KRAS phosphorylation was essential for survival and tumorigenic activity. Further, we identified phosphorylated KRAS in a panel of primary human pancreatic tumors. Taken together, our findings establish that KRAS requires S181 phosphorylation to manifest its oncogenic properties, implying that its inhibition represents a relevant target to attack KRAS-driven tumors.

Downloaded from cancerres.aacrjournals.org on January 7, 2014. © 2013 American Association for Cancer Research.

Author Manuscript Published OnlineFirst on December 26, 2013; DOI: 10.1158/0008-5472.CAN-13-1750
Author manuscripts have been peer reviewed and accepted for publication but have not yet been edited.

Introduction

RAS proteins are well-known small GTPases involved in the regulation of key signal transduction pathways. Cycling from the inactive (GDP-bound) to the active (GTP-bound) state faithfully responds to extracellular signals due to its tight regulation by GTP-exchange factors (GEFs) and GTPase activating proteins (GAPs). Activating point mutations that render RAS proteins insensitive to the extracellular signals are crucial steps in the development of the vast majority of cancers (1-3). Three different genes code for a total of four different Ras isoforms named HRAS, NRAS, KRAS4A and KRAS4B. *RAS* mutations, mainly at the *KRAS4B* (herein after referred to as *KRAS*) genes, occur in pancreatic (95%), colon (40%) and adenocarcinomas of the lung (35%) (1, 4, 5). The most prevalent oncogenic mutations in *RAS* at codons 12, 13 and 61 preserve the GTP-bound, active state by inhibiting intrinsic GTPase activity or interfering with the action of GAPs. In the GTP-bound form, RAS is able to interact with different effector proteins and consequently activates signal transduction pathways. Among those, the best characterized are the RAF1/MEK/ERK and the phosphatidylinositol-3-kinase (PI3K)/AKT (6, 7).

Since oncogenic mutations of *KRAS* give rise to an always GTP-bound protein which constitutively activates the effectors, positive or negative physiological regulation of oncogenic KRAS was not initially expected. Several reversible posttranslational modifications of KRAS have been described that could modulate KRAS oncogenic activity (8). Ubiquitination of oncogenic KRAS at lysine-147 in the guanine nucleotide-binding motif increases its binding to the downstream effectors PI3K and RAF1 thus increasing its tumorigenic activity (9). Furthermore, acetylation at lysine-104 affects interaction with GEFs and inhibits in vitro transforming activity of oncogenic KRAS (10). KRAS has, adjacent of the farnesylated C-terminal cysteine, a

Downloaded from cancerres.aacrjournals.org on January 7, 2014. © 2013 American Association for Cancer Research.

Author Manuscript Published OnlineFirst on December 26, 2013; DOI: 10.1158/0008-5472.CAN-13-1750
Author manuscripts have been peer reviewed and accepted for publication but have not yet been edited.

stretch of six contiguous lysines in a total of eight lysine residues -known as the polybasic domain- which promotes an electrostatic interaction with the negatively-charged phosphate groups of phospholipids (11, 12). Phosphorylation of KRAS at serine-181 within this domain has been described (13). We previously reported a role of KRAS Ser181 phosphorylation for activation of the wild-type KRAS in vitro and to regulate also in vitro oncogenic KRAS activity (14). By using both a genetic and pharmacological approach we demonstrate here that phosphorylation of oncogenic KRAS is required for tumor growth in vivo and that also this modification can be detected in human tumors. Furthermore, pharmacological inhibition of oncogenic KRAS phosphorylation suppresses KRAS oncogenic activity.

Materials and Methods

Antibodies and reagents

Primary antibodies used for immunoblotting were as follow: Anti-Actin (clone C4) (#691001; 1:1000; MP Biomedicals, Santa Ana, CA, USA), Anti-GAPDH (#MAB374; 1:1000; Chemicon, Billerica, MA, USA); Anti-cleaved caspase-3 (Asp175) (#9661; 1:1000; Cell Signaling, Danvers, MA, USA); Anti-AKT (#9272; Cell Signaling); Anti-phospho-AKT (Thr308) (#9275; 1:1000, Cell Signaling), Anti-p44/42 MAPK (ERK 1/2) (#9102; 1:1000; Cell Signaling); Anti-phospho-p44/42 MAPK (ERK 1/2) (Thr202/Tyr204) (#9101; 1:1000; Cell Signaling), Anti-cyclin B1 (#4138; 1:1000; Cell Signaling); Anti-KRAS (clone Ab-1) mouse (#OP24, 1:400, Calbiochem); Anti-Pan-Ras (clone Ab-3) mouse (#OP40; 1:400; Calbiochem); Anti-HRAS (clone C20) rabbit (#Sc-520, Santa Cruz); Anti-NRAS (clone F155) mouse (#Sc-31, Santa Cruz); Anti-GAP120 (sc-63; 1:100; Santa Cruz, Santa Cruz, CA, USA); Anti-PKCδ (#610398; 1:500; BD Transduction Laboratories, San Jose, CA); Anti-phospho-PKCδ

Downloaded from cancerres.aacrjournals.org on January 7, 2014. © 2013 American Association for Cancer Research.

Author Manuscript Published OnlineFirst on December 26, 2013; DOI: 10.1158/0008-5472.CAN-13-1750
Author manuscripts have been peer reviewed and accepted for publication but have not yet been edited.

(Ser643/676) (#9376; 1:1000; Cell Signaling). For immuhistochemistry we used Anti-Ki-67 (SP6) (#NM-9106S; 1:200; NeoMarkers, Kalamazoo, MI, USA). We used DeadEnd Colorimetric TUNEL System (G7132; Promega) for the TUNEL assays.

The reagents used for the detection of phospho-KRAS were: Protein Phosphatase λ (#539514-20KV; Calbiochem); Phos-tag™ (#AAL-107, Wako Chemicals GmbH, Neuss, Germany).

The inhibitors of PKC used were: Bryostatin-1 (#BIB0342, Apollo Scientific, Chesire, UK), Edelfosine (1-O-Octadecyl-2-O-methyl-glycero-3-phosphorylcholine) (#BML-L108, Enzo Life Science, Farmingdale, NY, USA), Bisindolylmaleimide I (BIM) (#CAS 176504-36, Millipore), Gö6983 (#G1918, Sigma Aldrich).

Cell lines

NIH3T3, SW480, A549, MPanc-96 and HPAF-II cells obtained from American Tissue and Cell Collection (ATCC) were grown in Dulbecco's Modified Eagle's Medium (DMEM) containing 10% FCS (Biological Industries), and routinely verified according to the specifications outlined in the ATCC Technical Bulletin. NIH3T3 stable cell lines expressing either HA-KRASG12V, HA-KRASG12V-S181A or HA-KRASG12V-S181D were obtained as previously described (14) .

DLD-1 knock-out of mutant KRAS allele DLD1$^{KRASwt/-}$ were obtained from Horizon Discovery Ltd (clone D-WT7; #HD105-002; http://www.horizondiscovery.com; Cambridge, UK). DLD1$^{KRASwt/-}$ cells were generated using the proprietary adeno-associated virus (AAV) gene targeting technology GENESIS®. Cells were maintained according to the supplier recommendations in McCoy's modified media containing 10% FBS (Biological Industries). DLD1$^{KRASwt/-}$ stable cell lines expressing either HA-KRASG12V, HA-KRASG12V-S181A or HA-KRASG12V-S181D were obtained from

Downloaded from cancerres.aacrjournals.org on January 7, 2014. © 2013 American Association for Cancer Research.

Author Manuscript Published OnlineFirst on December 26, 2013; DOI: 10.1158/0008-5472.CAN-13-1750
Author manuscripts have been peer reviewed and accepted for publication but have not yet been edited.

DLD1$^{KRASwt/-}$ after transfecting with the specific HA-KRASV12 plasmids (14) and a puromycine resistance plasmid (pSG5A). After selection with puromycine (4 µg/mL) clones or pools were obtained. .

Tumor generation in mice

The day of the injection, one million NIH 3T3 cells stably expressing either HA-KRASG12V, HA-KRASG12V-S181A or HA-KRASG12V-S181D suspended in 0,1 mL PBS buffer were subcutaneously injected into both flanks of Swiss nude mice (foxn1$^{-/-}$). Generated tumors were measured over time and at day 18 after injection, mice were euthanized and tumors were harvested, weighed, measured and processed for analysis (each group n=10).

For DLD-1 xenografts, one million cells stably expressing either HA-KRASG12V or HA-KRASG12V-S181A suspended in 0,1 mL PBS buffer were subcutaneously injected into both flanks of Swiss nude mice (foxn1$^{-/-}$). Generated tumors were measured over time and at day 28 after injection, mice were euthanized and tumors were harvested, weighed, measured and processed for analysis (each group n=10).

For the assays with the PKC inhibitors, one million NIH 3T3 cells stably expressing either HA-KRASG12V or HA-KRASG12V-S181D were subcutaneously injected into both flanks of Swiss nude mice. When tumor reached a designated volume of ~150 mm^3, animals were randomized and divided into vehicle (DMSO), Bryostatin-1 or Edelfosine treatment groups. Mice were weighed daily and received an intraperitoneal injection of either 75 µg/Kg Bryostatin-1 in 5% (v/v) DMSO, 30 mg/Kg Edelfosine in 5% (v/v) DMSO or 5% (v/v) DMSO (vehicle) for 5 days. At day 6 after the beginning of the treatment, mice were euthanized and tumors were harvested, weighed and processed for analysis.

Downloaded from cancerres.aacrjournals.org on January 7, 2014. © 2013 American Association for Cancer Research.

Author Manuscript Published OnlineFirst on December 26, 2013; DOI: 10.1158/0008-5472.CAN-13-1750
Author manuscripts have been peer reviewed and accepted for publication but have not yet been edited.

All mouse experiments were performed in accordance with protocols approved by the Animal Care and Use Committee of ICO-IDIBELL Hospitalet de Llobregat, Barcelona, Spain.

Sample Lysis, Gel electrophoresis, immunoblotting,

Cultured cells were lysed in Ras extraction buffer (20 mM Tris–HCl, pH 7.5, 2 mM EDTA, 100 mM NaCl, 5 mM $MgCl_2$, 1% (v/v) Triton X-100, 5 mM NaF, 10% (v/v) glycerol and 0.5% (v/v) 2-mercaptoethanol) supplemented with a cocktail of protease and phosphatase inhibitors (0.1 mM Na_3VO_4, 1 mM phenylmethylsulfonyl fluoride, 10 mM β-glycerophosphate, 2 μg/ml aprotinin and 10 μg/ml leupeptin)

Tumors were lysed using Polytron (Fischer Scientific, Pittsburg, PA, USA) in Ras extraction buffer, and protein resolved using standard SDS-PAGE electrophoresis. After electrotransfer, membranes were incubated using the indicated antibodies and then incubated with peroxidase-coupled secondary antibody. Immunocomplexes were detected by enhanced chemiluminescence reaction ECL western blotting analysis system (Amersham Biosciences, Piscataway, NJ, USA) and imaged by LAS-3000 (Fujifilm, Tokyo, Japan). When required, band intensity was determined using the measurement tool of Multigauge 2.0 (FUJIFILM, Tokyo, Japan).

Cell viability assay (MTT)

Human cell lines or DLD-1 expressing the same amounts of HA-KRASG12V and HA-KRASG12V-S181D were seeded at 10^4 cells per p96 with DMEM 10% FCS. Next day, were treated with the corresponding concentration of PKC inhibitors for 48h. Then, 10 μL of AB solution (MTT Cell Growth Assay Kit, #CT02, Millipore) were added to each well and incubated at 37ºC for 4h. Then, 0.1 mL isopropanol with 0.04 N HCl was

Downloaded from cancerres.aacrjournals.org on January 7, 2014. © 2013 American Association for Cancer Research.

Author Manuscript Published OnlineFirst on December 26, 2013; DOI: 10.1158/0008-5472.CAN-13-1750
Author manuscripts have been peer reviewed and accepted for publication but have not yet been edited.

added and mixed thoroughly. Absorbance was measured with a test wavelength of 570 nm and a reference wavelength of 630 nm according to manufacturer's recommendations.

Measurement of Ras isoform activation

RBD (Ras-binding domain of Raf-1) pull-down assays were performed as previously described (14) to determine the amount of active K-, H- and NRAS.

Histology

Mice tumors were embedded either in paraffin or frozen in OCT. Paraffin sections were stained following the haematoxylin-eosin standard protocol to study their histological appearance. Mitotic count in 5 consecutive high-power fields (100x) was performed to compare the mitotic index between groups. Frozen section in OCT were used to determine apoptosis by TUNEL assay following manufacturers recommendations (Roche), and to determine the percentage of proliferating cells by immunohistochemistry using Ki-67 antibodies.

Human tumors

Five biopsies of Human Pancreatic Ductal Adenorcarcinoma obtained by Doudenopancreatectomy were orthotopically implanted to nude mice and were perpetuated at least four passages. All patients gave informed written consent to participate and to have their biological specimens analyzed. The study was cleared by the Ethical Committee of Hospital de Bellvitge.

Detection of phospho-KRAS

Downloaded from cancerres.aacrjournals.org on January 7, 2014. © 2013 American Association for Cancer Research.

Author Manuscript Published OnlineFirst on December 26, 2013; DOI: 10.1158/0008-5472.CAN-13-1750
Author manuscripts have been peer reviewed and accepted for publication but have not yet been edited.

195 Phos-tag™ SDS-PAGE. To detect phospho-KRAS from human tumor samples and
196 from nude mice grafts, a fragment of ~ 0,1 g from a tumor biopsy was homogenized in
197 0,4 mL of λ Phosphatase Lysis Buffer (50 mM Tris-HCl pH 8; 150 mM NaCl, 2 mM
198 EDTA, 10% Glycerol, 1% Nonidet P40, 5 mM DTT, 2mM $MnCl_2$) containing either
199 protease inhibitor cocktail (Halt Protease Inhibitor Cocktail, #87786, Thermo Scientific,
200 Rockford, IL USA) alone or plus phosphatase inhibitors (0.2 mM Na_3VO_4, 5 mM NaF).
201 For human cell lines, a 10 cm dish was homogenized in the λ Phosphatase Lysis Buffer
202 as described above. Then, samples homogenized with only protease inhibitors were
203 treated with recombinant Protein Phosphatase λ for 30 minutes at 30ºC according to
204 manufacturer instructions, and finally all tubes were balanced with phosphatase
205 inhibitors in order to equalize both lysis buffers.
206 Protein content was assessed by Lowry method (Lowry et al, 1951) and tubes were
207 balanced. 10 µg protein were loaded into a 12%-polyacrilamide SDS-PAGE gel
208 supplemented with 100 µM Phos-tag™ and 100 µM $MnCl_2$ (according to Phos-tag™
209 SDS-PAGE protocol indicated by manufacters). The gel was run over night at 5 mA/gel
210 and soaked in a general transfer buffer containing 1 mM EDTA for 20 min followed by
211 10 minutes incubation with a transfer buffer without EDTA. Then, gels were transferred
212 over night at 50 V into a PDVF membrane that was blocked and blotted with anti-
213 KRAS (#OP24, Calbiochem).
214 Two-dimensional gel electrophoresis (2-DE). 100 µg of tumor extract prepared as
215 indicated above, were diluted to a final concentration of 7M urea, 2M thiourea, 4%
216 CHAPS {3-[(3-cholamidopropyl)-dimethylammonio]-1-propanesulfonate}, 65 mM
217 DTE, 0.1% ampholytes (Bio-Lyte 3/10, no. 163-1113; Bio-Rad) and 1.2% DestreakTM
218 Reagent (GE Healthcare, 17-6003-18) to 125 µL volume. Two-dimensional first-
219 dimension electrophoresis was performed as isoelectric focusing (IEF) with precast,

Downloaded from cancerres.aacrjournals.org on January 7, 2014. © 2013 American Association for Cancer Research.

Author Manuscript Published OnlineFirst on December 26, 2013; DOI: 10.1158/0008-5472.CAN-13-1750
Author manuscripts have been peer reviewed and accepted for publication but have not yet been edited.

220 immobilized pH gradient (IPG) gel strips (ReadyStripTM IPG Strip, 7 cm, pH 7 to 10;
221 no. 163-2005 [Bio-Rad]) by using a PROTEAN IEF system (Bio-Rad). Sample
222 application and rehydration of the strips were carried out using the active method (50 V
223 contant) according to the manufacturer's instructions (Bio-Rad). Next focusing was
224 performed at 8000 to 20000 V per hour. IEF gels were equilibrated for 10 min in a
225 buffer containing 6 M urea, 0.375 M Tris [pH 8.8], 2% SDS, 20% glycerol, and 2%
226 [wt/vol] DTE, and the second-dimension run was carried out in SDS-polyacrylamide
227 gels. After electrophoresis, gels were transferred to PDVF membranes (Millipore) and
228 immunoblotted with antibodies against KRAS
229
230 **Statistics**
231 All analyses were performed with GraphPad Prism 5.0. Data represent mean ± SEM.
232 Mann-Whitney test was used to analyze significance levels. Specific significance levels
233 are found in figure legends. $P < 0.05$ was considered significant.
234

Downloaded from cancerres.aacrjournals.org on January 7, 2014. © 2013 American Association for Cancer Research.

Author Manuscript Published OnlineFirst on December 26, 2013; DOI: 10.1158/0008-5472.CAN-13-1750
Author manuscripts have been peer reviewed and accepted for publication but have not yet been edited.

Results and Discussion

Oncogenic KRAS phosphorylation at Ser-181 is required for tumor growth

To test the prediction that phosphorylation at Ser181 of oncogenic KRAS was required to support tumor growth, NIH3T3 stable cell lines expressing similar levels of oncogenic HA-tagged G12V KRAS, namely HA-KRAS-G12V-S181 (S181), non-phosphorylatable HA-KRAS-G12V-S181A (S181A) or phosphomimetic HA-KRAS-G12V-S181D (S181D) (Fig. 1A) were subcutaneously injected into nude mice and tumor growth was monitored over time. Tumor formation was nearly abolished in cells expressing non-phosphorylatable S181A (Fig. 1B,C and tables S1 and S2). Furthermore, a dramatic increase in tumor growth was observed for phosphomimetic S181D mutant compared to the phosphorylatable S181. No tumor growth was observed when injecting NIH3T3 cells stably expressing wild-type HA-KRAS (Table S1), which confirmed that both engraftment and growth was driven by our oncogenic KRAS phosphomutants. Interestingly, in spite of the dramatic diminished growth of non phosphorylatable S181A derived tumors, KRAS oncoprotein was overexpressed in those tumors compared to the S181 or S181D derived tumors (Fig. 1D). This suggests that, during the process of tumor development, cells with higher expression of non-phosphorylatable KRAS are positively selected in an attempt to overcome the lower tumorogenic activity exhibited by this mutant. Similar results were obtained when injecting in nude mice two independently immortalized S181A clones with distinct expression levels. Again in S181A clones, tumor growth was highly compromised irrespectively of the KRAS protein expression level (Fig. S1).

The impaired tumor growth of the non-phosphorylatable S181 G12V mutant associated with a distinct histological pattern. S181A tumors were composed mostly by cells with

Downloaded from cancerres.aacrjournals.org on January 7, 2014. © 2013 American Association for Cancer Research.

Author Manuscript Published OnlineFirst on December 26, 2013; DOI: 10.1158/0008-5472.CAN-13-1750
Author manuscripts have been peer reviewed and accepted for publication but have not yet been edited.

an epithelioid appearance and with a significant lymphocytic infiltration (S181A 10.00 ± 1.08 lymphocytes per x100 field vs S181 2.25 ± 0.63 vs S181D 1.25 ± 0.25, $p<0.0001$) (Fig. 3 and Fig.S3). Of note, the same histology has been previously reported for sarcomas harboring the mild *KRAS* codon 13 mutations (15). In contrast, S181 and S181D derived sarcomas were composed of a fusocellular population showing a hemangiopericitoid patterns. The non-phosphorylatable S181A tumors had also a lower mitotic rate (S181A 4.00 ± 1.53 mitotic cells per x100 field vs 27.00 ± 4.12 for S181 vs 54.75 ± 4.99 for S181D, $p<0.0001$) and were the only tumors showing detectable levels of cleaved-caspase 3, a bona fide apoptosis marker (Fig. 1D and Fig S2A), together with a significant increase in TUNEL positive cells (Fig. 2A, B.). This is in accordance with the decreased resistance to apoptosis already reported in vitro for S181A compared to S181 and S181D oncogenic KRAS mutants (14). In agreement with the prediction of a stronger activity of KRAS upon phosphorylation, the phosphomimetic S181D derived tumors exhibited higher ERK and AKT activity (Fig. 1D), accompanied by a pronounced increase in the number of positive cells for the proliferative marker Ki-67 (Fig. 2A,B). Although mild increase in TUNEL positive cells was also observed in S181D compared to S181 tumors, S181A tumors were the ones exhibiting the highest degree of apoptosis. Intriguingly, S181A tumors showed higher cyclin B1 expression than the others (Fig. 1D) in line with the requirement of increased Cyclin B1 for apoptosis induction previously reported in several tumor cell lines (16-18). Moreover, Cyclin B1 overexpression has already been related to the mild transforming phenotype of codon 13 *KRAS* mutations in NIH3T3 models (15).

Thus, the impossibility of phosphorylating oncogenic KRAS dramatically changes growth pattern rendering activating mutations much less aggressive and demonstrating the relevance of this posttranslational modification in KRAS-driven transformation.

Downloaded from cancerres.aacrjournals.org on January 7, 2014. © 2013 American Association for Cancer Research.

Author Manuscript Published OnlineFirst on December 26, 2013; DOI: 10.1158/0008-5472.CAN-13-1750
Author manuscripts have been peer reviewed and accepted for publication but have not yet been edited.

PKC inhibitors diminish oncogenic KRAS-mediated tumor growth

The dependence of oncogenic KRAS on S181 phosphorylation makes oncogenic KRAS a putative target for protein kinase inhibitors. Since PKCs are considered to be the putative kinases for KRAS Ser181 phosphorylation (13, 19, 20) we tested whether treatment with two general PKC inhibitors that are clinically relevant (Bryostatin-1 and Edelfosine) (21-25) were able to revert tumor growth in a dephosphorylation-dependent manner.

Bryostatin-1 inhibits PKC activity when administrated in vitro at concentrations as low as 0.1 nM (21). In our experiments we used 75 μg/Kg, a dose that was previously used for in vivo PKC inhibition (26). As shown in Fig. 4B, Bryostatin-1 treatment significantly reduced tumor growth of S181 whereas no effect was evident on "non-dephosphorylatable" S181D tumors. Of note, we found that Bryostatin-1 treatment, in accordance to its general PKC inhibitor activity, efficiently downregulated both total and active PKCδ levels as previously described (21) (Fig. 4C). Tumor reduction with Bryostatin-1 treatment was associated with a decreased ERK activity that was specific for S181 phosphorylatable mutant. Moreover, apoptosis was induced as shown by an increase of cleaved caspase-3 levels and TUNEL positive cells (Fig. 4C,D and Fig. S2B). Concomitantly, cell proliferation was inhibited (Fig. 4D.) while cyclin B1 expression was increased (Fig. 4C). In this way, Bryostatin-1 treatment showed high specificity for the dephosphorylatable S181 tumors and interestingly, treatment of these tumors efficiently recapitulated the growth and signaling pattern of S181A tumors (21)shown in Fig.1. Concordantly, PKC inhibition did not affect growing and signaling pattern, nor increased apoptosis in the non-dephosphorylatable KRAS S181D tumors.

Downloaded from cancerres.aacrjournals.org on January 7, 2014. © 2013 American Association for Cancer Research.

Author Manuscript Published OnlineFirst on December 26, 2013; DOI: 10.1158/0008-5472.CAN-13-1750
Author manuscripts have been peer reviewed and accepted for publication but have not yet been edited.

To further confirm the striking results obtained with Bryostatin-1 treatment on mice we treated the same stable transfected NIH3T3 mice grafts with Edelfosine. This is an ether lipid analog to HMG with reported strong PKC inhibitor activity both in vitro (27, 28) and in vivo (29). As shown in Fig S4, we reproduced a significantly reduced tumor growth of S181 and again no significant effect was observed in "non-dephosphorylatable" S181D tumors.

Altogether, these results suggested that both Bryostatin-1 and Edelfosine, by blocking PCK activity, impair tumor growth inducing KRAS dephosphorylation and subsequent apoptosis. To formally prove this hypothesis, detection of KRAS phosphorylation was necessary. Since no suitable antibodies are available, we used the Phos-Tag™-based approach (30, 31) to determine the oncogenic KRAS phosphorylation status in the generated tumors. This method is based on the fact that a complex formation between the phosphate group of a phosphorylated protein and a divalent metal ion in Phos-Tag™ reduces the mobility of the phospho-protein during the electrophoresis separation, thus allowing resolution of phosphorylated and non-phosphorylated proteins into different bands. As shown in Fig. 4E, a slow migrating band of HA-KRAS could be observed in the tumors generated from cells expressing the S181 oncogenic KRAS, that was absent in S181D tumors. Disappearance of this band upon λ Phosphatase treatment corroborated it was phosphorylated KRAS. Most interestingly, in Bryostatin-1 and Edelfosine treated animals phosphorylated KRAS was no longer observed (Fig.4E and Fig.S4). Together, these observations reinforce the notion that PKC-dependent Ser181-phosphorylation of oncogenic KRAS is required for tumorigenesis. This effect may account for the previously reported inhibition of different KRAS-driven tumor xenografts by PKC pharmacologic inhibition (29, 32, 33). Interestingly, it has also been

Downloaded from cancerres.aacrjournals.org on January 7, 2014. © 2013 American Association for Cancer Research.

Author Manuscript Published OnlineFirst on December 26, 2013; DOI: 10.1158/0008-5472.CAN-13-1750
Author manuscripts have been peer reviewed and accepted for publication but have not yet been edited.

shown that PKCδ knock-down prevents apoptosis and promotes tumorigenesis in cells addicted to aberrant KRAS signaling (34-36).

Human cell lines require phosphorylation of KRAS for survival and tumor growth

In order to determine whether the requirement for KRAS phosphorylation observed in our NIH3T3 KRAS-transformation model was also involved in human cell lines tumorigenesis, we ectopically expressed the HA-KRAS-G12V phosphomutants described above in the human colorectal cancer cell line DLD-1 but previously knocked-out for the oncogenic endogenous KRAS allele ($DLD1^{KRASwt/-}$).

We found that under serum-saturating growth conditions (10%FCS), human colon cancer cells DLD-1 expressing S181A mutant exhibited a significantly reduced growth compared to phosphomimetic S181D expressing cells (Fig. 5A). Trying to recapitulate tumor growth conditions, we evaluated cell growth under serum-limiting conditions (0.1% FCS). After 4 days of starvation, cells stably expressing S181A showed significantly higher reduced growth under serum starvation culture conditions compared to S181 and phosphomimetic S181D (Fig. 5A,). Moreover, S181A exhibited increased sensitivity to apoptosis under serum deprivation or by adriamycin- induced genotoxic damage (Fig 5A,B), thus demonstrating a pro-apoptotic effect of the S181A oncogenic KRAS.

In order to evaluate real tumorigenic capacity of these cells, subcutaneous injection of $DLD1^{KRASwt/-}$ expressing either HA-KRASG12V or HA-KRASG12V-S181A phosphomutants was performed. S181A derived tumors were significantly smaller than S181 tumors (Fig. 5C). This confirmed the requirement of KRAS S181 phosphorylation for tumorigenesis of human colon cell lines.

Downloaded from cancerres.aacrjournals.org on January 7, 2014. © 2013 American Association for Cancer Research.

Author Manuscript Published OnlineFirst on December 26, 2013; DOI: 10.1158/0008-5472.CAN-13-1750
Author manuscripts have been peer reviewed and accepted for publication but have not yet been edited.

A preferential activation of endogenous wild-type H- and N- RAS alleles induced by the oncogenic KRAS has recently been reported (37). To check whether diminished growth capacity of S181A was due to lack of activation of the endogenous RAS isoforms, RBD pull-down assays were performed to test GTP loading of endogenous RAS isoforms. Lower GTP loading of endogenous Ras in the S181A expressing cells was not observed compared with the other phosphomutants (Fig. S5).

Next, we wanted to determine whether BIM and Gö6983, two PKC inhibitors (38, 39) were able to affect DLD-1 cells in a KRAS S181-specific manner. To this aim, dose-response to these PKC inhibitors was evaluated in DLD1$^{KRASwt/-}$ cells expressing HA-KRASG12V and using DLD-1 expressing HA-KRASG12V-S181D as a non-dephosphorylatable control. After 48h of treatment, it was shown that at doses between 1μM and 20μM for BIM and 1.5μM and 10μM for Gö6983, cells expressing oncogenic KRAS with S181 exhibited significantly enhanced sensitivity to PKC inhibition compared to the phosphomimetic non-dephosphorylatable mutant (Fig 6A). Most importantly, after PKC inhibition, S181 cells lost its KRAS phosphorylation as shown by Phos-tag^{TM} SDS-PAGE gels (Fig 6A).

Finally, we evaluated the ability of a set of PKC inhibitors to reduce proliferation together with KRAS phosphorylation in a panel of human cell lines from different origin harboring oncogenic KRAS. We found that at doses reported to inhibit PKC (21, 28, 38, 40), cell growth was compromised. Most importantly, after 12h of treatment, band corresponding to phospho-KRAS was lost, thus reinforcing the idea that PKC inhibition is able to revert growth in a KRAS S181-dependent manner (Fig. 6B).

KRAS is phosphorylated in human tumors.

Downloaded from cancerres.aacrjournals.org on January 7, 2014. © 2013 American Association for Cancer Research.

Author Manuscript Published OnlineFirst on December 26, 2013; DOI: 10.1158/0008-5472.CAN-13-1750
Author manuscripts have been peer reviewed and accepted for publication but have not yet been edited.

Next, we investigated whether the S181 phosphorylation observed in our model system was also present in human tumors. To do so, a set of orthotopic xenografts derived from carcinomas of the exocrine pancreas were analyzed. Five tumors harboring codon 12 KRAS mutations were tested. As shown in Fig. 7, by using Phos-Tag™ SDS-PAGE, several bands were detected in all tumors using the anti-KRAS antibody. Treatment with λ phosphatase (Fig. 7) and two-dimensional electrophoresis analysis corroborated the presence of phosphorylated KRAS in these human tumors (Fig. S6). Thus, the presence of phospho-KRAS in human malignancies emphasizes the alleged requirement of this modification for human KRAS-driven tumorigenesis.

Altogether, the results depict a scenario of a novel tight regulation of KRAS oncogenicity by phosphorylation at S181. We have recently shown that although phosphorylated KRAS is mainly found at the plasma membrane (40, 41), phosphorylated K-Ras forms distinct plasma membrane signaling platforms that induce preferential activation of main KRAS effectors involved in oncogenesis . Interestingly, this distinct functionality could be reverted by PKC inhibitors (40). This would give a rationale for the strikingly different tumorigenic activity of oncogenic KRAS according to its S181 phosphorylation status .

The fact that, as we show, this could be efficiently pharmacologically inhibited raises the possibility of novel therapeutic strategies targeting KRAS-driven human malignancies. So far, clinical trials with PKC regulators have been disappointing mostly because of the lack of selectivity and unacceptable toxicity (39). The identification of KRAS as a key PKC target may help in developing specific inhibitors of KRAS phosphorylation.

Downloaded from cancerres.aacrjournals.org on January 7, 2014. © 2013 American Association for Cancer Research.

Author Manuscript Published OnlineFirst on December 26, 2013; DOI: 10.1158/0008-5472.CAN-13-1750
Author manuscripts have been peer reviewed and accepted for publication but have not yet been edited.

405

406 **Grant Support**

407 This study was supported by MICINN-Spain [SAF2010-20712]. Carles Barceló and

408 Noelia Paco are recipient of pre-doctoral fellowships from MEC-Spain, and the Catalan

409 Government respectively.

410

Downloaded from cancerres.aacrjournals.org on January 7, 2014. © 2013 American Association for Cancer Research.

Author Manuscript Published OnlineFirst on December 26, 2013; DOI: 10.1158/0008-5472.CAN-13-1750
Author manuscripts have been peer reviewed and accepted for publication but have not yet been edited.

411

412 References

413 1. Bos JL. Ras oncogenes in human cancer: A review. Cancer Res 1989;49:4682-9.

414 2. Malumbres M, Barbacid M. RAS oncogenes: The first 30 years. Nat Rev Cancer
415 2003;3:459-65.

416 3. Downward J. Control of ras activation. Cancer Surv 1996;27:87-100.

417 4. Prior IA, Lewis PD, Mattos C. A comprehensive survey of ras mutations in cancer.
418 Cancer Res 2012;72:2457-67.

419 5. Schubbert S, Shannon K, Bollag G. Hyperactive ras in developmental disorders and
420 cancer. Nat Rev Cancer 2007;7:295-308.

421 6. Shields JM, Pruitt K, McFall A, Shaub A, Der CJ. Understanding ras: 'It ain't over 'til
422 it's over'. Trends Cell Biol 2000;10:147-54.

423 7. Marshall CJ. Ras effectors. Curr Opin Cell Biol 1996;8:197-204.

424 8. Ahearn IM, Haigis K, Bar-Sagi D, Philips MR. Regulating the regulator: Post-
425 translational modification of RAS. Nat Rev Mol Cell Biol 2011;13:39-51.

426 9. Sasaki AT, Carracedo A, Locasale JW, Anastasiou D, Takeuchi K, Kahoud ER, et al.
427 Ubiquitination of K-ras enhances activation and facilitates binding to select downstream
428 effectors. Sci Signal 2011;4:ra13.

429 10. Yang MH, Nickerson S, Kim ET, Liot C, Laurent G, Spang R, et al. Regulation of
430 RAS oncogenicity by acetylation. Proc Natl Acad Sci U S A 2012;109:10843-8.

Downloaded from cancerres.aacrjournals.org on January 7, 2014. © 2013 American Association for Cancer Research.

Author Manuscript Published OnlineFirst on December 26, 2013; DOI: 10.1158/0008-5472.CAN-13-1750
Author manuscripts have been peer reviewed and accepted for publication but have not yet been edited.

11. Hancock JF, Magee AI, Childs JE, Marshall CJ. All ras proteins are polyisoprenylated but only some are palmitoylated. Cell 1989;57:1167-77.

12. Silvius JR. Mechanisms of ras protein targeting in mammalian cells. J Membr Biol 2002;190:83-92.

13. Ballester R, Furth ME, Rosen OM. Phorbol ester- and protein kinase C-mediated phosphorylation of the cellular kirsten ras gene product. J Biol Chem 1987;262:2688-95.

14. Alvarez-Moya B, Lopez-Alcala C, Drosten M, Bachs O, Agell N. K-Ras4B phosphorylation at Ser181 is inhibited by calmodulin and modulates K-ras activity and function. Oncogene 2010;29:5911-22.

15. Guerrero S, Figueras A, Casanova I, Farre L, Lloveras B, Capella G, et al. Codon 12 and codon 13 mutations at the K-ras gene induce different soft tissue sarcoma types in nude mice. FASEB J 2002;16:1642-4.

16. Yuan J, Yan R, Kramer A, Eckerdt F, Roller M, Kaufmann M, et al. Cyclin B1 depletion inhibits proliferation and induces apoptosis in human tumor cells. Oncogene 2004;23:5843-52.

17. Chu R, Terrano DT, Chambers TC. Cdk1/cyclin B plays a key role in mitotic arrest-induced apoptosis by phosphorylation of mcl-1, promoting its degradation and freeing bak from sequestration. Biochem Pharmacol 2012;83:199-206.

18. Borgne A, Versteege I, Mahe M, Studeny A, Leonce S, Naime I, et al. Analysis of cyclin B1 and CDK activity during apoptosis induced by camptothecin treatment. Oncogene 2006;25:7361-72.

Downloaded from cancerres.aacrjournals.org on January 7, 2014. © 2013 American Association for Cancer Research.

Author Manuscript Published OnlineFirst on December 26, 2013; DOI: 10.1158/0008-5472.CAN-13-1750
Author manuscripts have been peer reviewed and accepted for publication but have not yet been edited.

453 19. Bivona TG, Quatela SE, Bodemann BO, Ahearn IM, Soskis MJ, Mor A, et al. PKC
454 regulates a farnesyl-electrostatic switch on K-ras that promotes its association with bcl-
455 XL on mitochondria and induces apoptosis. Mol Cell 2006;21:481-93.

456 20. Alvarez-Moya B, Barcelo C, Tebar F, Jaumot M, Agell N. CaM interaction and
457 Ser181 phosphorylation as new K-ras signaling modulators. Small GTPases 2011;2:99-
458 103.

459 21. Choi SH, Hyman T, Blumberg PM. Differential effect of bryostatin 1 and phorbol
460 12-myristate 13-acetate on HOP-92 cell proliferation is mediated by down-regulation of
461 protein kinase cdelta. Cancer Res 2006;66:7261-9.

462 22. Gajate C, Matos-da-Silva M, Dakir e, Fonteriz RI, Alvarez J, Mollinedo F.
463 Antitumor alkyl-lysophospholipid analog edelfosine induces apoptosis in pancreatic
464 cancer by targeting endoplasmic reticulum. Oncogene 2012;31:2627-39.

465 23. Abraham I, El Sayed K, Chen ZS, Guo H. Current status on marine products with
466 reversal effect on cancer multidrug resistance. Mar Drugs 2012;10:2312-21.

467 24. Lopez-Campistrous A, Song X, Schrier AJ, Wender PA, Dower NA, Stone JC.
468 Bryostatin analogue-induced apoptosis in mantle cell lymphoma cell lines. Exp Hematol
469 2012;40:646,56.e2.

470 25. Biberacher V, Decker T, Oelsner M, Wagner M, Bogner C, Schmidt B, et al. The
471 cytotoxicity of anti-CD22 immunotoxin is enhanced by bryostatin 1 in B-cell
472 lymphomas through CD22 upregulation and PKC-betaII depletion. Haematologica
473 2012;97:771-9.

Downloaded from cancerres.aacrjournals.org on January 7, 2014. © 2013 American Association for Cancer Research.

Author Manuscript Published OnlineFirst on December 26, 2013; DOI: 10.1158/0008-5472.CAN-13-1750
Author manuscripts have been peer reviewed and accepted for publication but have not yet been edited.

474 26. Mohammad RM, Li Y, Mohamed AN, Pettit GR, Adsay V, Vaitkevicius VK, et al.
475 Clonal preservation of human pancreatic cell line derived from primary pancreatic
476 adenocarcinoma. Pancreas 1999;19:353-61.

477 27. Conesa-Zamora P, Mollinedo F, Corbalan-Garcia S, Gomez-Fernandez JC. A
478 comparative study of the effect of the antineoplastic ether lipid 1-O-octadecyl-2-O-
479 methyl-glycero-3-phosphocholine and some homologous compounds on PKC alpha and
480 PKC epsilon. Biochim Biophys Acta 2005;1687:110-9.

481 28. Zhou X, Arthur G. 1-O-octadecyl-2-O-methylglycerophosphocholine inhibits
482 protein kinase C-dependent phosphorylation of endogenous proteins in MCF-7 cells.
483 Biochem J 1997;324:897-902.

484 29. Liou JS, Chen JS, Faller DV. Characterization of p21Ras-mediated apoptosis
485 induced by protein kinase C inhibition and application to human tumor cell lines. J Cell
486 Physiol 2004;198:277-94.

487 30. Kinoshita E, Kinoshita-Kikuta E, Koike T. Separation and detection of large
488 phosphoproteins using phos-tag SDS-PAGE. Nat Protoc 2009;4:1513-21.

489 31. Van Itallie CM, Tietgens AJ, LoGrande K, Aponte A, Gucek M, Anderson JM.
490 Phosphorylation of claudin-2 on serine 208 promotes membrane retention and reduces
491 trafficking to lysosomes. J Cell Sci 2012;125:4902-12.

492 32. Jasinski P, Welsh B, Galvez J, Land D, Zwolak P, Ghandi L, et al. A novel
493 quinoline, MT477: Suppresses cell signaling through ras molecular pathway, inhibits
494 PKC activity, and demonstrates in vivo anti-tumor activity against human carcinoma
495 cell lines. Invest New Drugs 2008;26:223-32.

Downloaded from cancerres.aacrjournals.org on January 7, 2014. © 2013 American Association for Cancer Research.

Author Manuscript Published OnlineFirst on December 26, 2013; DOI: 10.1158/0008-5472.CAN-13-1750
Author manuscripts have been peer reviewed and accepted for publication but have not yet been edited.

496 33. Jasinski P, Zwolak P, Terai K, Borja-Cacho D, Dudek AZ. PKC-alpha inhibitor
497 MT477 slows tumor growth with minimal toxicity in in vivo model of non-ras-mutated
498 cancer via induction of apoptosis. Invest New Drugs 2011;29:33-40.

499 34. Xia S, Chen Z, Forman LW, Faller DV. PKCdelta survival signaling in cells
500 containing an activated p21Ras protein requires PDK1. Cell Signal 2009;21:502-8.

501 35. Shen L, Kim SH, Chen CY. Sensitization of human pancreatic cancer cells
502 harboring mutated K-ras to apoptosis. PLoS One 2012;7:e40435.

503 36. Symonds JM, Ohm AM, Carter CJ, Heasley LE, Boyle TA, Franklin WA, et al.
504 Protein kinase C delta is a downstream effector of oncogenic K-ras in lung tumors.
505 Cancer Res 2011;71:2087-97.

506 37. Jeng HH, Taylor LJ, Bar-Sagi D. Sos-mediated cross-activation of wild-type ras by
507 oncogenic ras is essential for tumorigenesis. Nat Commun 2012;3:1168.

508 38. Pal D, Outram SP, Basu A. Upregulation of PKCeta by PKCepsilon and PDK1
509 involves two distinct mechanisms and promotes breast cancer cell survival. Biochim
510 Biophys Acta 2013;1830:4040-5.

511 39. Mochly-Rosen D, Das K, Grimes KV. Protein kinase C, an elusive therapeutic
512 target? Nat Rev Drug Discov 2012;11:937-57.

513 40. Barcelo C, Paco N, Beckett AJ, Alvarez-Moya B, Garrido E, Gelabert M, et al.
514 Oncogenic K-ras segregates at spatially distinct plasma membrane signaling platforms
515 according to its phosphorylation status. J Cell Sci 2013;126:4553-9.

Downloaded from cancerres.aacrjournals.org on January 7, 2014. © 2013 American Association for Cancer Research.

Author Manuscript Published OnlineFirst on December 26, 2013; DOI: 10.1158/0008-5472.CAN-13-1750
Author manuscripts have been peer reviewed and accepted for publication but have not yet been edited.

516 41. Lopez-Alcala C, Alvarez-Moya B, Villalonga P, Calvo M, Bachs O, Agell N.
517 Identification of essential interacting elements in K-ras/calmodulin binding and its role
518 in K-ras localization. J Biol Chem 2008;283:10621-31.

519
520

Downloaded from cancerres.aacrjournals.org on January 7, 2014. © 2013 American Association for Cancer Research.

Author Manuscript Published OnlineFirst on December 26, 2013; DOI: 10.1158/0008-5472.CAN-13-1750
Author manuscripts have been peer reviewed and accepted for publication but have not yet been edited.

Figure Legends

Fig. 1. Phosphorylation at Ser181 is necessary for tumor growth of oncogenic KRAS-G12V. NIH 3T3 cells stably expressing either, HA-KRAS-G12V (S181), HA-KRAS-G12V-S181A (S181A) or HA-KRAS-G12V-S181D (S181D) were injected into each flank of nude mice (each group n=10). A) Levels of exogenous HA-KRAS from the different NIH 3T3 pools were analyzed by immunoblot the day of injection into mice. Pool S181#2 was injected into mice (herein after referred to as S181); B) Tumor volumes were measured at days 13, 16 and 19 after injection; C) At day 19 mice were euthanized and tumors were dissected and weighed. Graph showing the weight of excised tumors (each dot corresponds to a tumor); D) Total cell lysates of representative excised tumors were immunoblotted to detect the indicated proteins (numbers indicate different tumors). Anti-GAP120 was used as loading control;

Fig. 2. Lack of growth of non-phospohorylatable KRAS tumors correlates with decreased proliferation (Ki-67) and increased apoptosis (TUNEL) markers. A) Tumor sections were stained for Ki-67 or TUNEL. Scale bars represent 50 μm;B) Quantifications of Ki-67 labeling (left) and TUNEL labeling (right) were made from at least 2 different tumors per mutant (each point represents a counted field). (***, $p<0.0001$, **, $p<0.001$ and *, $p<0.01$, p for Student's two-tailed t test; mean and SEM are represented).

Fig. 3. Differential tumor growth according to KRAS phosphorylation is associated with a distinct histological patern. Paraffin sections were stained following the haematoxylin-eosin protocol to study their histological appearance. Arrow caps indicate lymphocyte infiltration. Scale bars represent 50 μm.

Fig. 4. Pharmacologic inhibition of PKC activity inhibits tumor growth and KRAS-G12V dependent signaling pathways in a K-RasG12V Ser181-phosphorylation dependent manner. NIH 3T3 cells stably expressing either HA-KRAS-G12V (S181); or HA-KRAS-G12V-S181D (S181D) were injected into each flank of nude mice. When tumor reached a designated volume of ~150 mm^3 (latency time shorter for S181D tumors), animals were divided into two groups (each group n=10) and treated daily either with vehicle (5% DMSO) or Bryostatin-1 (Bryo) (75 μg/Kg) for 6 days, and euthanized next day. **A)** Western blot showing HA-K-Ras

Downloaded from cancerres.aacrjournals.org on January 7, 2014. © 2013 American Association for Cancer Research.

Author Manuscript Published OnlineFirst on December 26, 2013; DOI: 10.1158/0008-5472.CAN-13-1750
Author manuscripts have been peer reviewed and accepted for publication but have not yet been edited.

552 expression in different pools of NIH 3T3 cells the day of injection. Injected NIH 3T3
553 pools (red arrows) were chosen among the ones with equivalent expression for HA-
554 KRAS-G12V (S181) or HA-KRAS-G12V-S181D (S181D); **B)** Increment in tumor size
555 was obtained by comparing tumor volume at the starting day (day 1) and at day 7 of
556 treatment. Dissected tumors from the nude mice are displayed below the graph. Scale
557 bar represents 25 mm **C)** Total cell lysates of representative excised tumors were
558 immunoblotted to detect the indicated proteins (numbers indicate different tumors).
559 Anti-GAP120 was used as loading control **D)** Quantifications of Ki-67 labeling (left)
560 and TUNEL labeling (right) were made from at least 2 different tumors per mutant
561 (each point represents a counted field). (***, $p<0.0001$, **, $p<0.001$ and *, $p<0.01$, p
562 value for Student's two-tailed t test; ns: non-significant differences; mean and SEM are
563 represented). **E)** Cellular extract from tumors were resolved in Phos-Tag^{TM} SDS-PAGE
564 gels and immunoblot was performed using anti-HA antibody. An aliquot of a S181
565 tumor from an animal treated with DMSO was incubated, prior to electrophoresis, at
566 30ºC with phosphatase λ (λ) or only with buffer (Ctl) to discard unspecific effects due to
567 heating samples.

568 **Fig. 5**. **Phosphorylation at Ser181 is necessary for cell proliferation, survival and**
569 **tumor growth of DLD1 $^{KRAS\ wt/-}$ cell expressing KRASG12V phosphomutants.** A)
570 $3{\cdot}10^4$ DLD1 $^{KRAS\ wt/-}$ cells stably expressing either HA-KRASG12V-S181A, HA-
571 KRASG12V-S181D or HA-KRASG12V-S181 were cultured under serum-saturated
572 (10% FCS) or serum-limiting (0.1% FCS) conditions for 4 days and counted to evaluate
573 the proliferation rate. KRAS expression of the different mutants at the initial day and
574 levels of cleaved caspase 3 (Cl. casp 3) at the fourth day are showed. B) The different
575 mutants were cultured for 2 days with adryamicin (5μM) to induce genotoxic damage.
576 The sensitivity to apoptosis was analyzed by the levels of cleaved caspase 3 (Cl. casp
577 3). C) Pools of DLD1 $^{KRAS\ wt/-}$ expressing HA-KRAS-G12V S181 or HA-KRAS-G12V
578 S181A were injected into each flank of nude mice. Levels of exogenous HA-KRAS
579 from the pools injected were analyzed by immunoblot the day of injection into mice. At
580 day 28 after injection mice were euthanized and tumors were weighed. Graph showing
581 the weight of excised tumors.

582

Downloaded from cancerres.aacrjournals.org on January 7, 2014. © 2013 American Association for Cancer Research.

Author Manuscript Published OnlineFirst on December 26, 2013; DOI: 10.1158/0008-5472.CAN-13-1750
Author manuscripts have been peer reviewed and accepted for publication but have not yet been edited.

583 **Fig.6. Pharmacologic PKC inhibition impairs KRAS phosphorylation and cell**
584 **survival.** A) DLD1 $^{KRAS\ wt/-}$ expressing KRASG12V -S181 or KRASG12V-S181D (as
585 non-dephosphorylatable control) were treated with the PKC inhibitors Gö6938 (Gö)
586 (1.5, 5 and 10 μM) and BIM (1, 10 and 20 μM) for 48 hours. The columns represent
587 the growth rate estimated by the measurement of the absorbance following the MTT
588 assay as a function of the initial cell number (left). Extracts from DLD1 KRAS wt/-
589 expressing KRASG12V -S181 or KRASG12V-S181D treated or no with phosphatase λ
590 (λ) or with PKC inhibitors (Gö6983 or BIM) were resolved in Phos-Tag™ SDS-PAGE
591 gel following by immunoblotting using anti-KRAS antibodies (right).**B)** A pannel of
592 human cell lines from different origin harboring oncogenic KRAS were treated with 5
593 μM BIM, 1 μM Gö6983 (Gö), 1 μM Bryostatin-1(Bryo) and 10 μg/mL Edelfosine
594 (Edelf) for 48h. Cells were harvested and extracts were resolved in Phos-Tag™ SDS-
595 PAGE and immunoblotted using anti-KRAS antibody.

596 **Fig. 7. Detection of the phosphorylated form of oncogenic KRAS in human**
597 **pancreatic ductal adenocarcinomas.** Extract from 5 different human pancreatic ductal
598 adenocarcinomas with oncogenic mutations in codon 12 of KRAS (#1 G12D
599 heterozygous; #2 G12D heterozygous; #3 G12D homozygous; #4 G12V heterozygous;
600 #5 G12V heterozygous), were resolved in Phos-Tag™ SDS-PAGE or SDS-PAGE
601 followed by immunoblotting using anti-KRAS antibodies. An aliquot of each extract
602 was previously incubated with phosphatase λ. Anti-GAP120 was used as loading
603 control.

Downloaded from cancerres.aacrjournals.org on January 7, 2014. © 2013 American Association for Cancer Research.

Author Manuscript Published OnlineFirst on December 26, 2013; DOI: 10.1158/0008-5472.CAN-13-1750
Author manuscripts have been peer reviewed and accepted for publication but have not yet been edited.

Fig 1

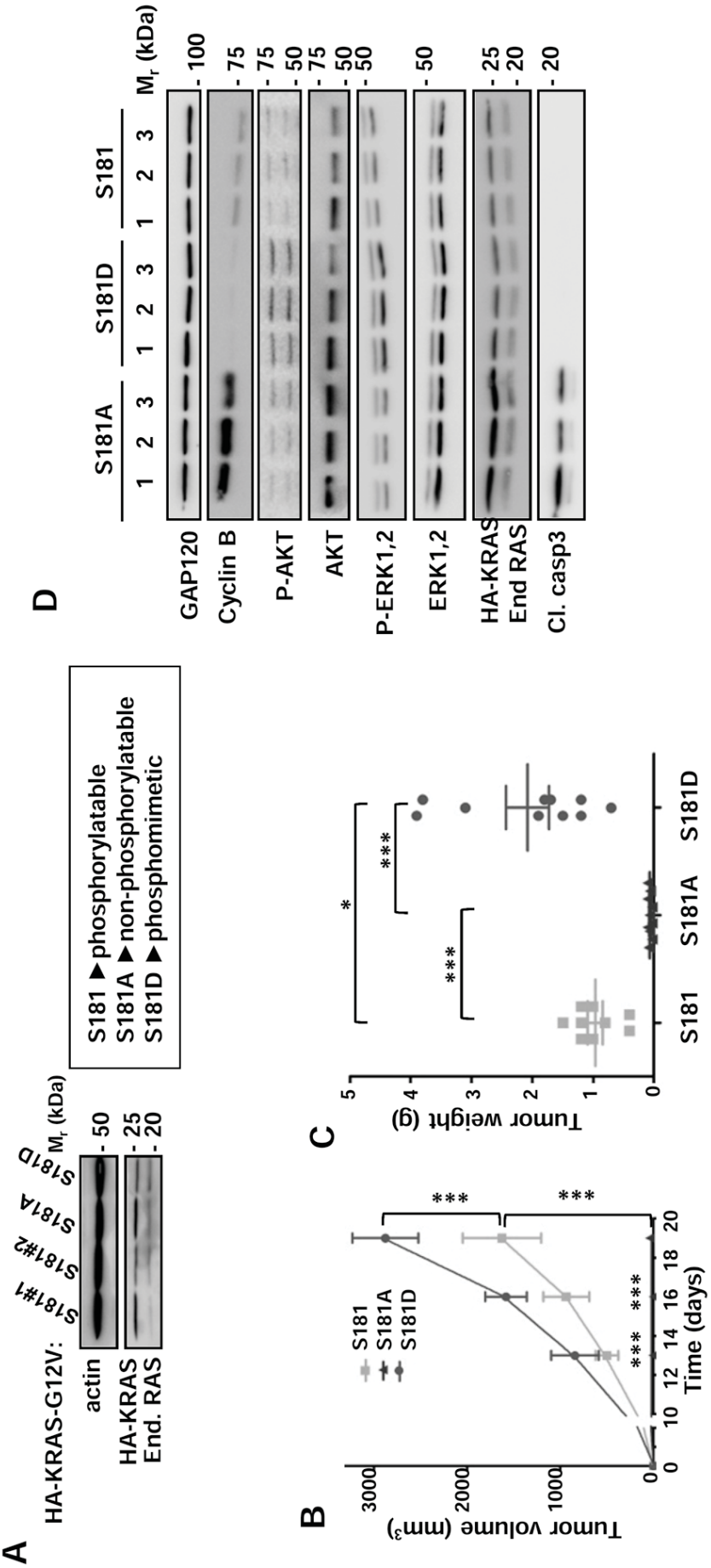

Downloaded from cancerres.aacrjournals.org on January 7, 2014. © 2013 American Association for Cancer Research.

Author Manuscript Published OnlineFirst on December 26, 2013; DOI: 10.1158/0008-5472.CAN-13-1750
Author manuscripts have been peer reviewed and accepted for publication but have not yet been edited.

Fig 2

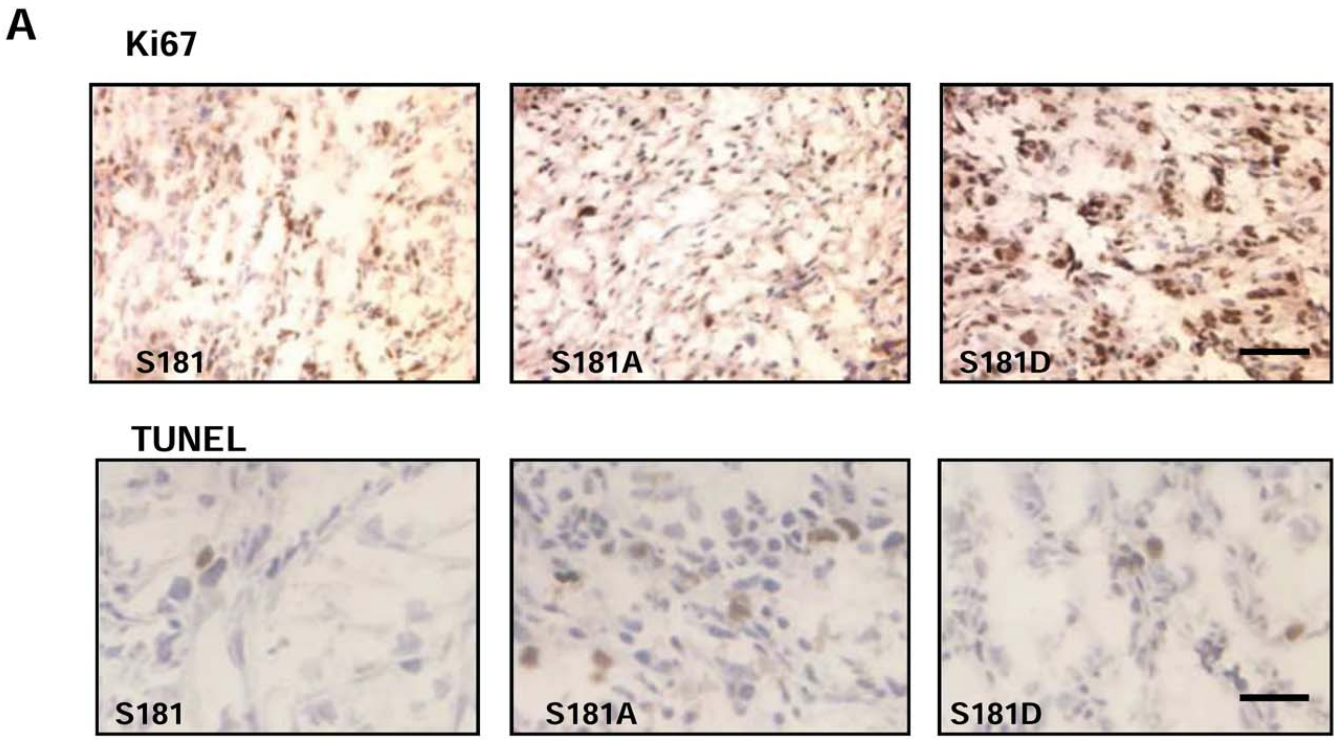

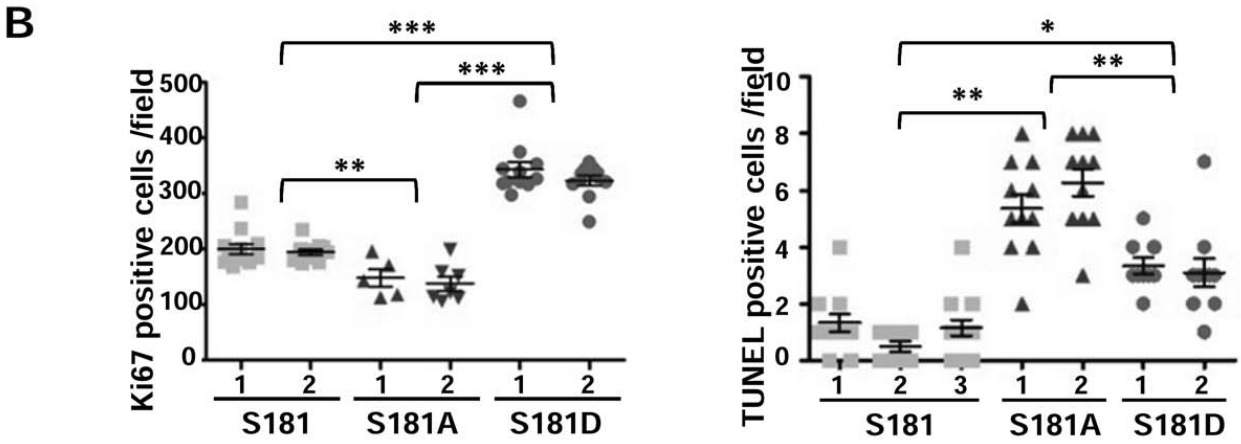

Downloaded from cancerres.aacrjournals.org on January 7, 2014. © 2013 American Association for Cancer Research.

Author Manuscript Published OnlineFirst on December 26, 2013; DOI: 10.1158/0008-5472.CAN-13-1750
Author manuscripts have been peer reviewed and accepted for publication but have not yet been edited.

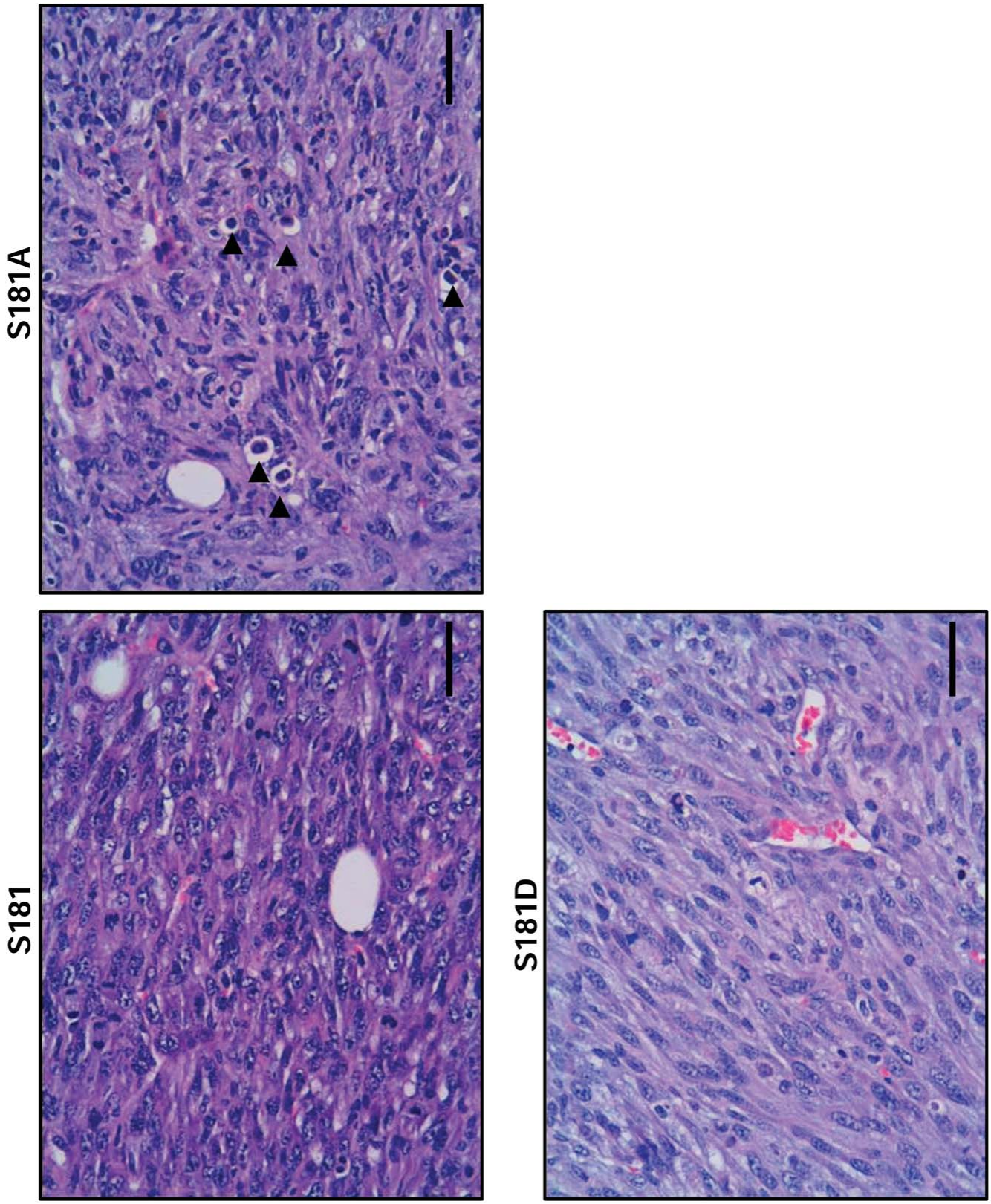

Fig 3

Downloaded from cancerres.aacrjournals.org on January 7, 2014. © 2013 American Association for Cancer Research.

Author Manuscript Published OnlineFirst on December 26, 2013; DOI: 10.1158/0008-5472.CAN-13-1750
Author manuscripts have been peer reviewed and accepted for publication but have not yet been edited.

Fig 4

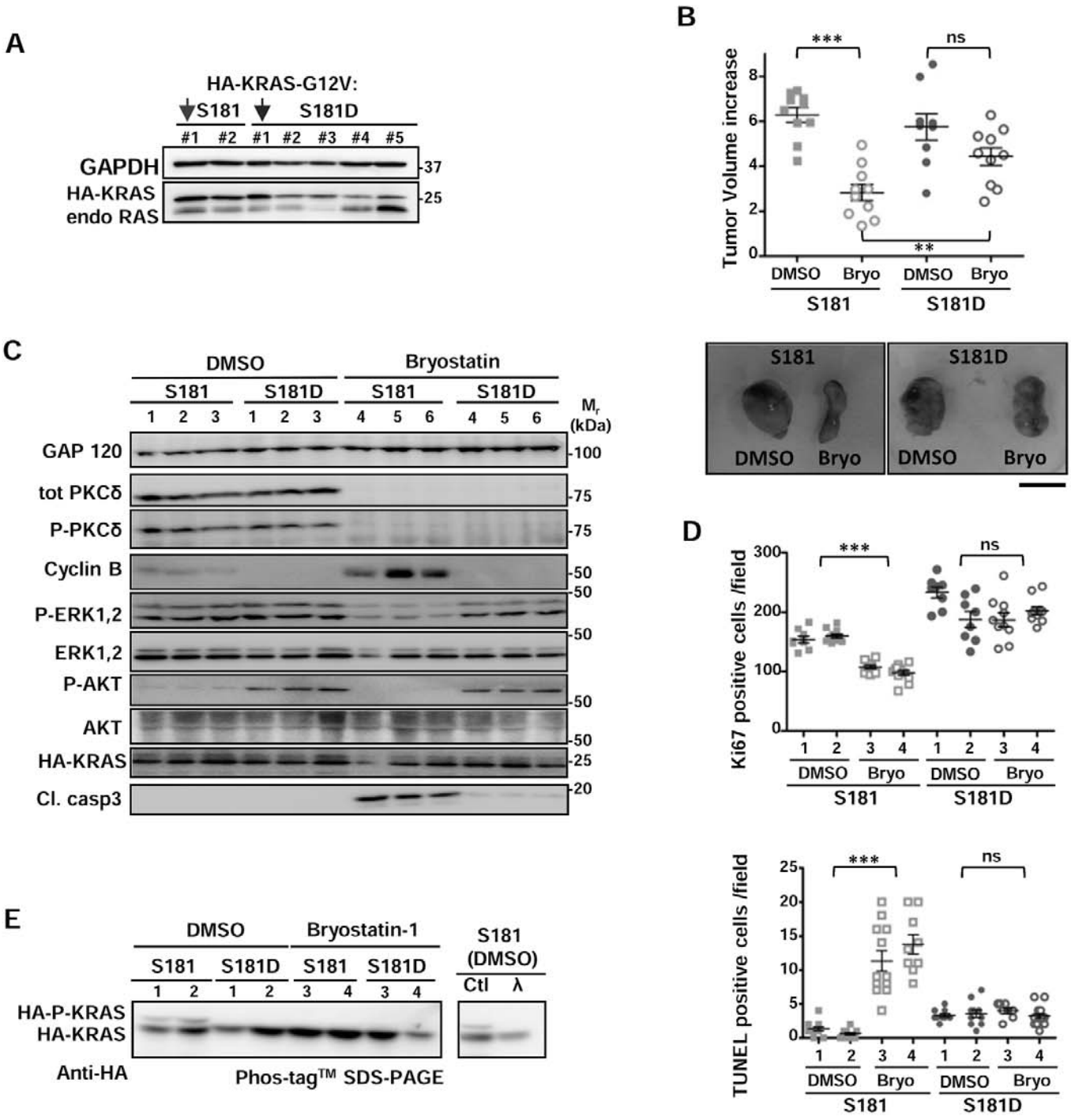

Downloaded from cancerres.aacrjournals.org on January 7, 2014. © 2013 American Association for Cancer Research.

Author Manuscript Published OnlineFirst on December 26, 2013; DOI: 10.1158/0008-5472.CAN-13-1750
Author manuscripts have been peer reviewed and accepted for publication but have not yet been edited.

Fig 5

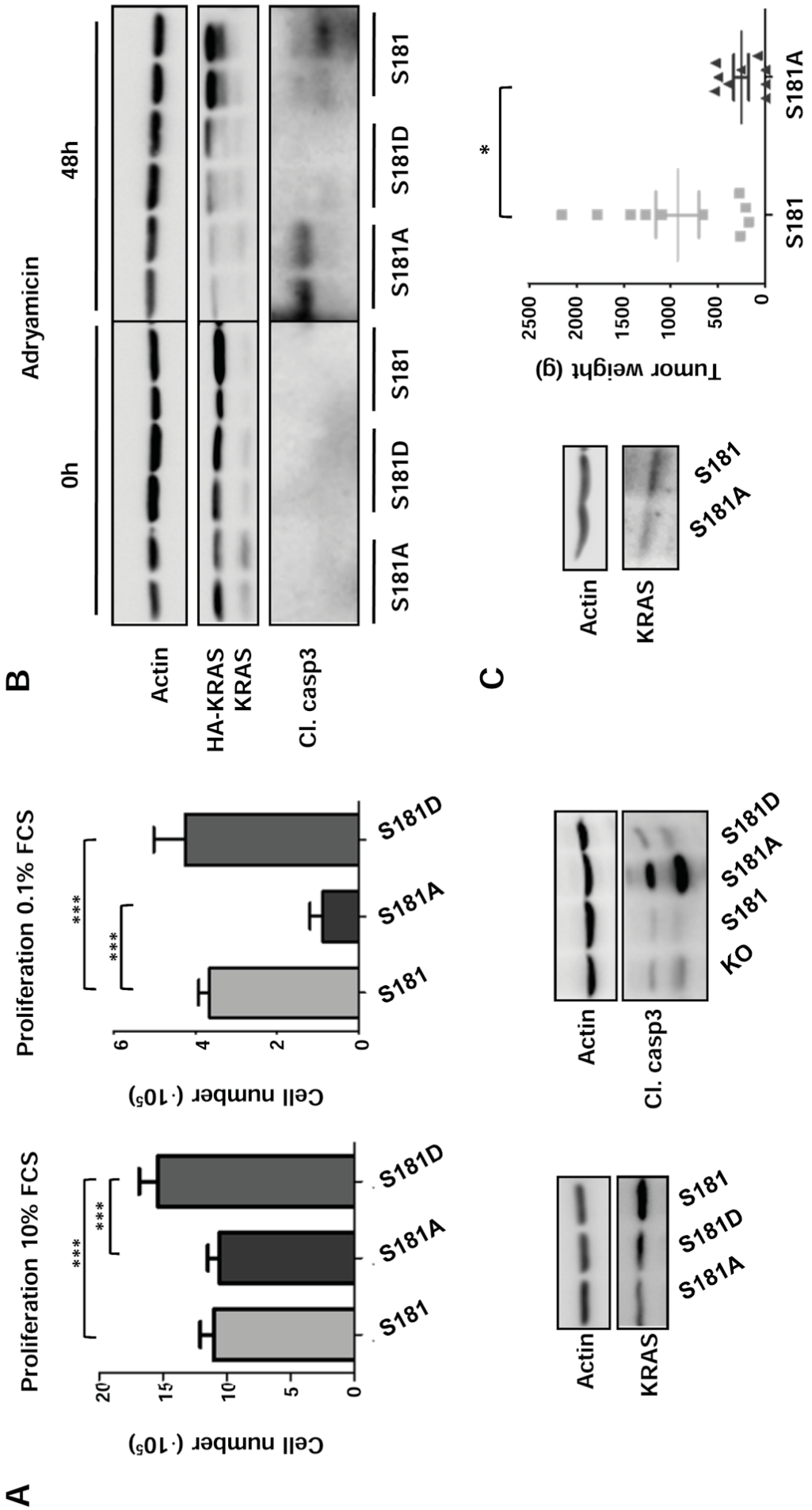

Downloaded from cancerres.aacrjournals.org on January 7, 2014. © 2013 American Association for Cancer Research.

Author Manuscript Published OnlineFirst on December 26, 2013; DOI: 10.1158/0008-5472.CAN-13-1750
Author manuscripts have been peer reviewed and accepted for publication but have not yet been edited.

Fig 6

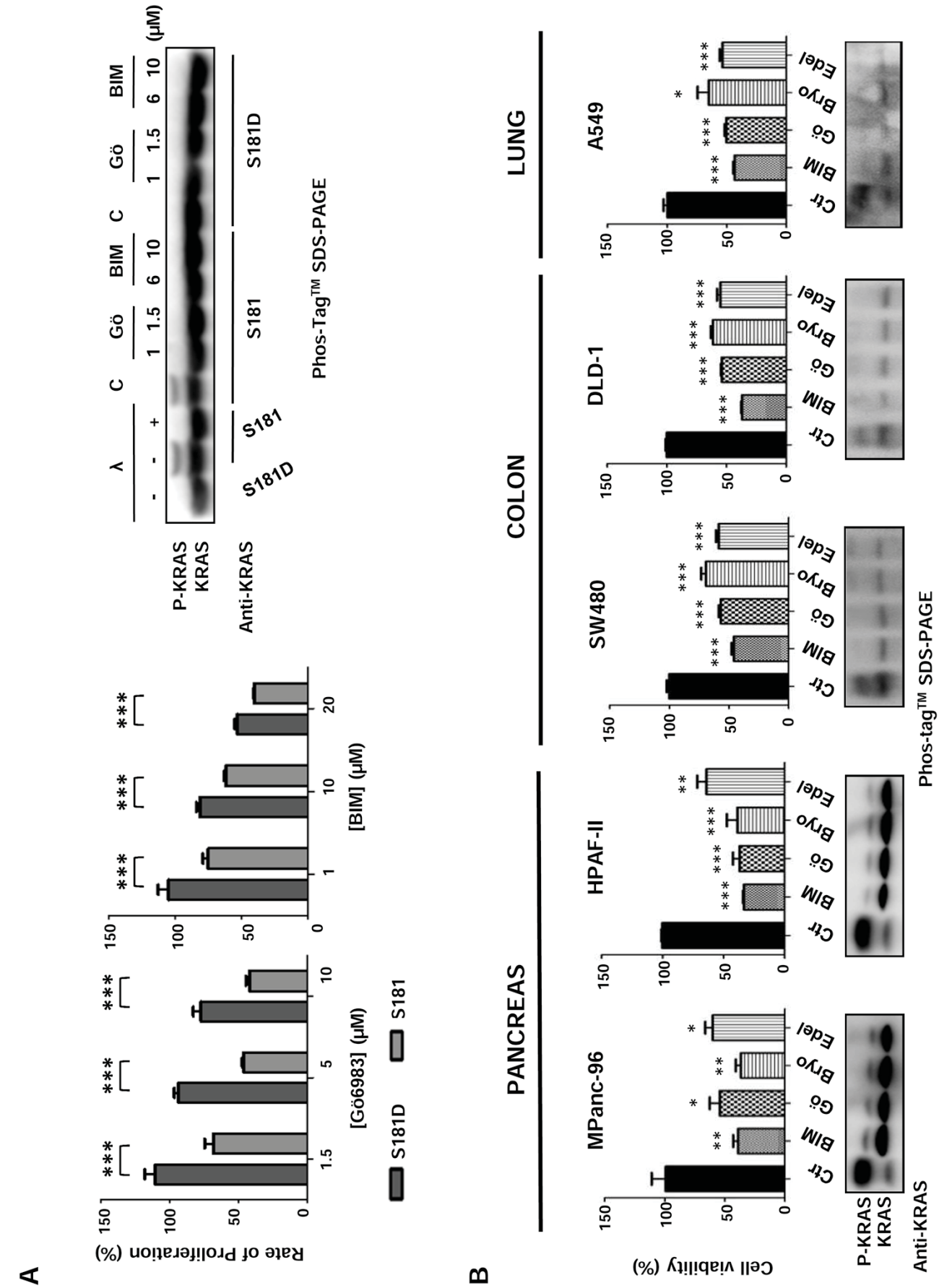

Downloaded from cancerres.aacrjournals.org on January 7, 2014. © 2013 American Association for Cancer Research.

Author Manuscript Published OnlineFirst on December 26, 2013; DOI: 10.1158/0008-5472.CAN-13-1750
Author manuscripts have been peer reviewed and accepted for publication but have not yet been edited.

Fig 7

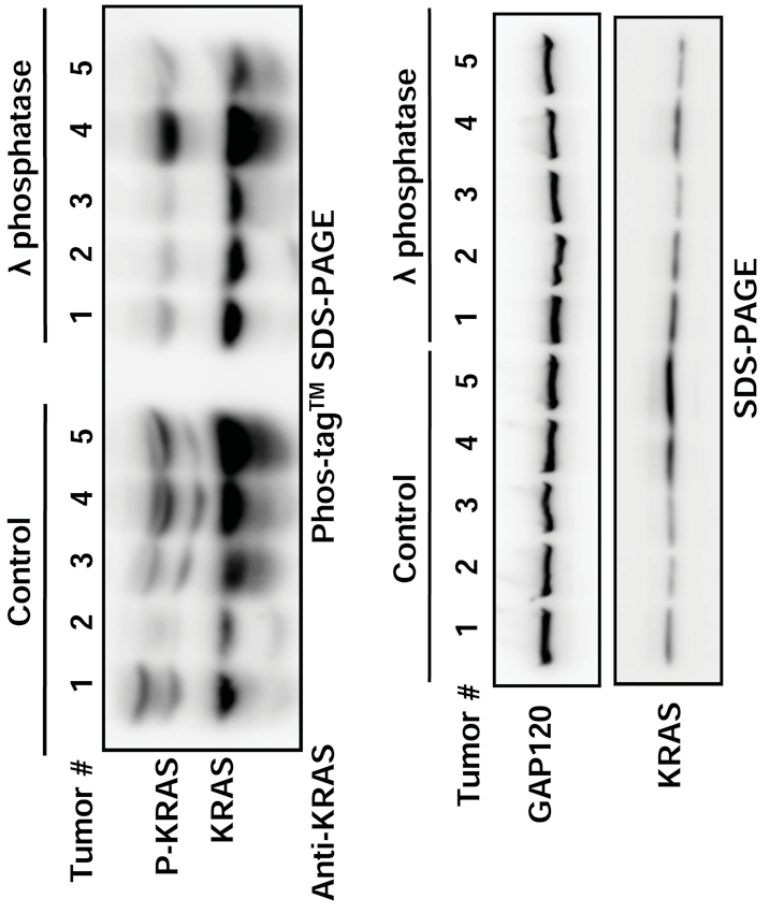

Downloaded from cancerres.aacrjournals.org on January 7, 2014. © 2013 American Association for Cancer Research.